Ecology, 88(8), 2007, pp. 2058–2071
© 2007 by the Ecological Society of America

SPECTRAL ANALYSIS UNMASKS SYNCHRONOUS AND COMPENSATORY DYNAMICS IN PLANKTON COMMUNITIES

David A. Vasseur[1,3] and Ursula Gaedke[2]

[1]*Department of Biology, McGill University, 1205 Ave. Docteur Penfield, Montreal, Quebec H3A 1B1 Canada*
[2]*Universität Potsdam, Institut für Biochemie und Biologie, Am Neuen Palais 10, D-14469 Potsdam, Germany*

Abstract. Community biomass is often less variable than the biomasses of populations within the community, yet attempts to implicate compensatory dynamics between populations as a cause of this relationship often fail. In part, this may be due to the lack of appropriate metrics for variability, but there is also great potential for large-scale processes such as seasonality or longer-term environmental change to obscure important dynamics at other temporal scales. In this study, we apply a scale-resolving method to long-term plankton data, to identify the specific temporal scales at which community-level variability is influenced by synchrony or compensatory dynamics at the population level. We show that variability at both the population and community level is influenced strongly by a few distinct temporal scales: in phytoplankton, ciliate, rotifer, and crustacean communities, synchronous dynamics are predominant at most temporal scales. However, in phytoplankton and crustacean communities, compensatory dynamics occur at a sub-annual scale (and at the annual scale in crustaceans) leading to substantial reductions in community-level variability. Aggregate measures of population and community variability do not detect compensatory dynamics in these communities; thus, resolving their scale dependence unmasks dynamics that are important for community stability in this system. The methods and results presented herein will ultimately lead to a better understanding of how stability is achieved in communities.

Key words: community; population; portfolio effect; spectral analysis; time series; variability.

Introduction

It has been established that the temporal variability of an ecological character, such as biomass, can largely depend upon the organization level at which it is measured (e.g., at the population vs. community level). Investigating what conditions lead to a reduction, or an increase in the variability at one level, relative to another, has become a central issue in ecology. Most prominently featured has been the importance of diversity at the population level; communities are expected to exhibit less temporal variability as population diversity increases (Doak et al. 1998, Tilman et al. 1998, McCann 2000, Loreau et al. 2002). Hypothetically, this result arises because greater population-level diversity increases the probability of having functionally complementary populations in a community, which provides buffering against environmental stresses or disturbance (Yachi and Loreau 1999). However, theoretical work describing the influence of diversity on population- and community-level variability has outpaced experimental evidence (Hooper et al. 2005) and what evidence is available suggests that the relationship is not unequivocal (Cottingham et al. 2001). Long-term experiments and field research assessing temporal stability (variability) across organizational levels have been identified as areas deserving of further attention (Hooper et al. 2005).

Functional complementarity in communities is manifested as a process known as compensation (Micheli et al. 1999). Compensation, or compensatory dynamics, describes a balancing process within the community that is achieved when the decline of some populations is offset by the increase of others. This leads to a reduction in community-level variability relative to the opposing case, when populations fluctuate in synchrony. Tilman (1996) was perhaps the first to demonstrate compensatory dynamics in an experimental system and many studies have followed in pursuit of compensatory dynamics (e.g., Klug et al. 2000, Fischer et al. 2001; for reviews see Micheli et al. 1999 and Cottingham et al. 2001). It has also been shown that in diverse communities, compensatory dynamics are not required to reduce community-level variability relative to the population level. Rather, such a relationship may arise when population fluctuations are independent (Doak et al. 1998); the independent fluctuations that are visible at the population level become less evident at the community level because increased richness converges the community biomass toward its mean. This relationship was first known by economists as the "portfolio

Manuscript received 14 November 2006; accepted 11 December 2006; final version received 10 January 2007. Corresponding Editor: L. Stone.

[3] Present address: Department of Biological Sciences, University of Calgary, Calgary, Alberta T2N 1N4 Canada. E-mail: dvasseur@ucalgary.ca

effect," where a diverse portfolio leads to less volatility in one's total assets.

Detecting compensatory dynamics in natural systems requires a suitable metric with which to compare variability (Micheli et al. 1999). The temporal variance σ^2 is unsuitable for directly comparing the variability among populations and between populations and communities because it scales with mean biomass as a power-law ($\sigma^2 \propto \mu^z$) where z often falls between 1 and 2 (Murdoch and Stewart-Oaten 1989). Two measures of variability, the standard deviation (or variance) of log-transformed data, SD(log[X]), and the coefficient of variation, CV, are independent of the mean when $z = 2$ (McArdle et al. 1990). While the former measure is less sensitive to differences in population means when $z \neq 2$ (Cottingham et al. 2001), it is plagued by the need to replace or omit zeroes (McArdle et al. 1990), which are often encountered when biomass falls below the detection threshold of the methods employed.

A second, but potentially larger challenge withstanding the detection of compensatory dynamics in natural systems arises from spatiotemporal scale (Levin 1992, Micheli et al. 1999, Cottingham et al. 2001). Increasing the scale of measurement increases the estimated temporal variability of populations and communities (Pimm and Redfearn 1988) but may also lead to the inclusion of two or more scales at which populations have different dynamic relationships, thus obfuscating the true variability relationships (Micheli et al. 1999, Keitt and Urban 2005). For example, populations may oscillate simultaneously and independently at more than one scale (Van Voris et al. 1980, Grover et al. 2000, Vasseur et al. 2005), generating dynamics that are synchronous at one temporal scale yet compensatory at another (Keitt and Fischer 2006). This property can easily confound the detection of either relationship when employing traditional analytical techniques (see example in *Methods*), and important small-scale phenomena may be hidden by more obvious large-scale patterns (Levin 1992).

To overcome the challenges involved in detecting compensatory dynamics in nature we combine the use of log transformed data collected from four plankton communities, with a scale-resolving method for estimating the variability of populations and communities. By comparing our results against a "null" model (those results which we attribute to the portfolio effect), we identify the specific temporal scales at which community-level variability is influenced by synchrony or compensatory dynamics amongst populations. We determine the temporal scales and population dynamics that are important for community-level variability in four plankton communities in Lake Constance and we compare our results with previous and concurrent studies of plankton variability in Lake Constance (Gaedke et al. 1996, Huber and Gaedke 2006; U. Gaedke, *unpublished manuscript*) and other systems.

METHODS

Spectral analysis and scale-dependent population dynamics

Populations which express compensatory changes in response to some environmental factor will, when summed into a community, vary less than populations which express synchronous changes in response to the same factor (provided that biomass is distributed relatively evenly). We introduce a simple contrived example to show how compensatory dynamics at one temporal scale can be obscured by synchronous dynamics at another scale, and how spectral analysis can reveal the scale-dependencies of variability relationships.

Consider a community (C) of $n = 2$ populations (P_1 and P_2), each with equal mean density μ, and two periodic components with frequencies f_1 and f_2. The populations and community vary through time according to the following expressions:

$$P_i(t) = \mu + \alpha\sin(2\pi f_1 t) + \alpha\sin(2\pi f_2 t - 2\pi i/N) + \xi_i(t)$$

$$C(t) = \sum_i^N P_i(t). \quad (1)$$

where $i = 1 \ldots N$. The noise term $\xi_i(t)$ is drawn randomly from a normal distribution (μ_ξ, σ_ξ^2). The harmonic model above provides a contrived but useful example of population dynamics; not only do populations vary at fixed scales (similar to annual variability in temperate systems, or tidal variability in marine and intertidal systems), synchronous and compensatory dynamics can be easily generated by manipulating the phases of sinusoidal components. Phase is simply a measure of the temporal shift in the oscillation, which causes the sinusoidal oscillation to peak at an earlier or later time. In the model in Eq. 1, the phase of the first periodic component (f_1) is zero for all n populations which leads them to oscillate in synchrony. The phase of the second periodic component differs among populations which leads them to exhibit compensatory dynamics (declines in some populations are always offset by increases in others). In the following paragraphs, and in Figs. 1 and 2, we will use this example to show how synchronous and compensatory population dynamics can be inferred from the spectrum of population and community time-series without knowledge of the underlying model.

Spectral analysis enables data measured over time (or another axis such as space) to be represented as the sum of many sine waves of different frequency. In the spectrum, each frequency explains a portion of the temporal variance of the process; a process that oscillates in time at a fixed frequency will have a large portion of its variance explained by this frequency. We show the utility of the spectrum for this study using the example below and we provide the particulars of generating the spectrum in a later section.

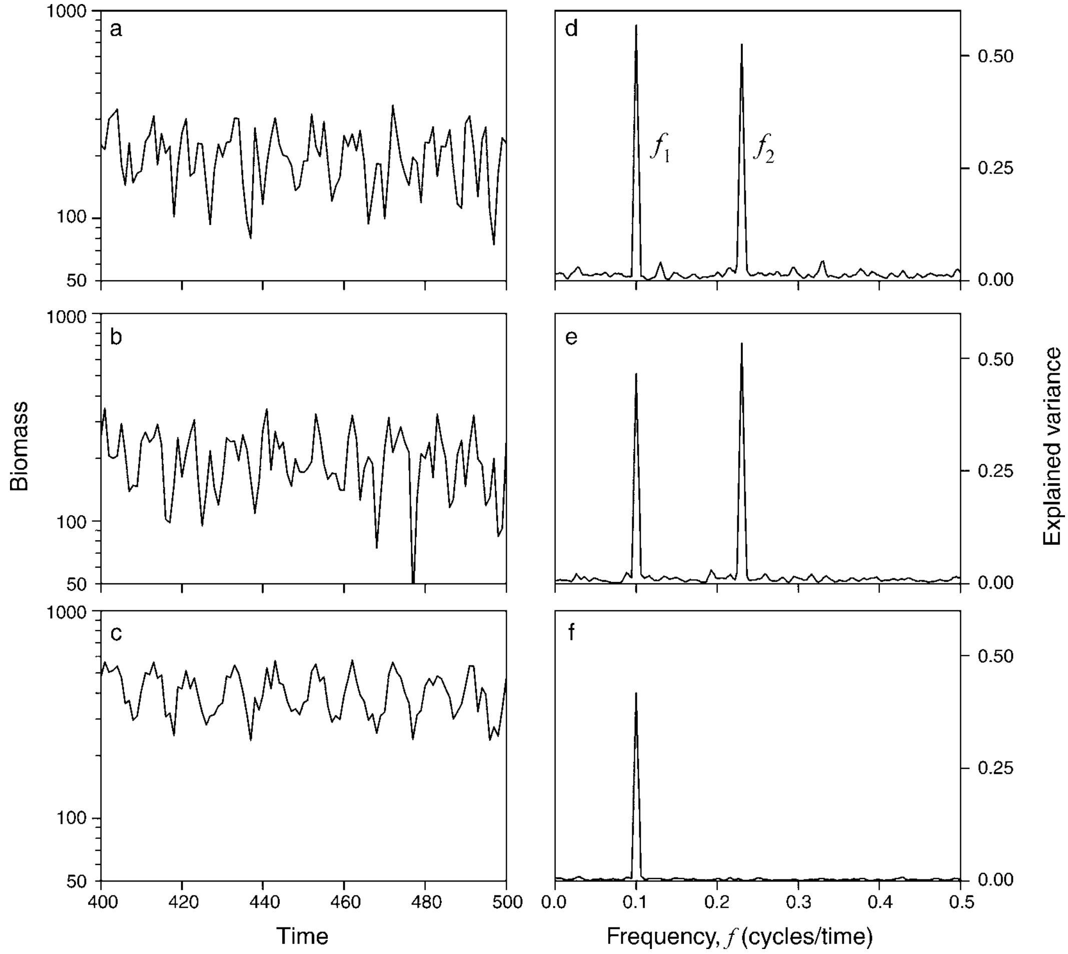

FIG. 1. Time series of (a, b) population and (c) community biomass generated by Eq. 1 for the parameters $\mu = 200$, $\alpha = 50$, $f_1 = 0.1$, $f_2 = 0.23$, $\mu_\varepsilon = 0$, and $\sigma_\varepsilon^2 = 40$ (note log scale). (d–f) Population dynamics (panels a and b) are synchronized at f_1 and compensatory at f_2.The associated spectra show the amount of temporal variance of the log-transformed time-series explained by each frequency; the amount of explained variance at frequency f_i is proportional to the reduction in the sum of squares that is achieved by removing a periodic component with frequency f_i from the time series.

Fig. 1a–c shows the time series of the two populations and the community respectively, simulated using Eq. 1, and Fig. 1d–f shows their associated spectra. We log-transform the population and community time series prior to computing the spectrum to account for the mean–variance rescaling relationship; the community mean is twice the mean of each population whereas the community variance is four times the variance of each population. The population spectra (Fig. 1d, e) are nearly identical, and show both populations varying at two frequencies with nearly equal amplitude. Fig. 1d, e provide information about the amplitude of periodic components but not about their phases and thus we cannot determine the presence of synchronous or compensatory population dynamics from them alone. However, comparing the community spectrum (Fig. 1f) to the population spectra we notice strong coherence at f_1, while the peak at frequency f_2 is absent. From this we can infer that the population dynamics are synchronous at f_1, given that the amount of explained variance is approximately equal in the community and population spectra (recall that data are log-transformed, so equal variance is expected). We can also infer that the population dynamics are compensatory at f_2, given that the amount of explained variance is largely reduced in the community spectrum when compared to the population spectra. Had we simply measured the cross-correlation of these two populations ($\hat{\rho}_{P_1P_2} = -0.05$) the functional relationship that generates synchrony and compensation at fixed temporal scales would be obscured.

One hurdle to applying the above logic to real data is the extension from two to many populations; comparing the spectra in a pair-wise fashion becomes quickly unfeasible with growing n. However, this problem can be overcome by comparing a single "mean" population spectrum to the community spectrum. Consider a second example constructed using Eq. 1 but this time

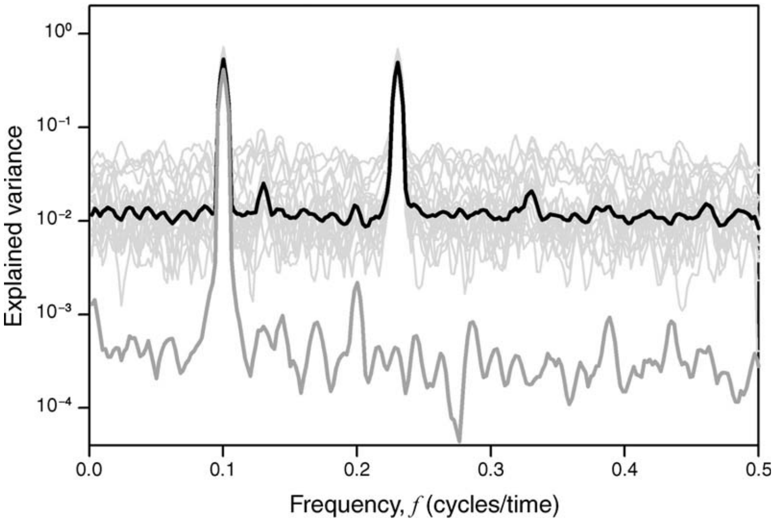

FIG. 2. The population spectra (light gray lines), mean population spectrum (black line), and community spectrum (heavy gray line) generated by Eq. 1 for a community of $N = 20$ populations using the same parameters as in Fig. 1 and log-transformed data. The 20 populations all differ in phase at the second frequency (f_2), culminating as compensatory population dynamics. "Explained variance" is shown on a logarithmic scale to highlight the reduction in variance that occurs across all frequencies and particularly at f_2, where compensatory dynamics occur.

with $n = 20$. Again, all populations again exhibit synchronous dynamics at f_1 but at the second periodic component f_2 they each have slightly different phases (and thus exhibit compensatory dynamics). Fig. 2 shows the spectra of each population, the geometric mean population spectrum, which is independently calculated at each frequency (we use the geometric mean since the population spectra are log-normally distributed on the y-axis), and the community spectrum. Again, these spectra relate only information about the amplitude of fluctuations, not their phases, and so the "mean spectrum" shows only which scales are the most important sources of population temporal variability. Since both the mean population and community spectra exhibit large amounts of explained variance at f_1 we infer that population dynamics are synchronous at this temporal scale. The absence of the second periodic component f_2 from the community spectrum allows us to infer that compensatory dynamics occur at this temporal scale. Here we have shown the "explained variance" on a logarithmic scale to highlight the importance of Portfolio effects; frequency-independent fluctuations are damped at the community level and can be easily observed as the reduction in explained variance that is common to all "background" frequencies.

Data acquisition

Lake Constance (Bodensee) is a large (473 km^2) and deep ($\bar{z} = 101$ m) temperate lake located at approximately 47°40′ N, 9°20′ E and bordered by Germany, Switzerland, and Austria. The lake is monomictic and mesotrophic. Plankton samples were taken from the Northwestern arm of the lake over the period 1979 to 1999 with an uneven sampling frequency. Organisms were taxonomically resolved to species level (or to a higher level where necessary) at the time of counting and converted to units of carbon based upon empirical relationships (Müller et al. 1991, Gaedke 1998, Straile and Geller 1998, Gaedke et al. 2002). We constructed time series of biomass for each species (or higher taxa), which we herein refer to as populations. For each of the four major plankton groups (which we herein refer to as communities): phytoplankton, ciliates, rotifers, and crustaceans (see Plate 1); we constructed a total biomass time series by summing the population biomasses at each sampling event. Table 1 provides details on the number of taxonomic groups within each plankton community (richness) in addition to specific details on the sampling period and sample size for each.

Spectral analysis

Traditional methods of spectral analysis rely on a Fourier transformation of the time-series data. However, this transformation precludes data which are not sampled at a fixed interval. Long-term ecological data is often sampled irregularly due to changing short-term objectives or seasonal unavailability. Traditionally, researchers have treated this problem by interpolating missing points or by "re-binning" data into equally spaced groups; however, the former technique generally performs poorly for long gaps in the data (Press et al. 2001), and the latter limits estimation of the spectrum in the high frequency range (Schulz and Stattegger 1997).

Driven by a similar problem in astrophysical records, Lomb (1976) developed a method of estimating the periodogram for unevenly sampled data, which was later

TABLE 1. Aspects of Lake Constance plankton data sets.

Community	Date range	No. sampling events	Richness (n)	Unevenness (a)†
Phytoplankton	1979–1999	836	36	0.33
Ciliates	1987–1998	455	25	0.28
Rotifers	1984–1996‡	427	21	0.51
Crustaceans	1979–1998	759	7	0.70

† The parameter a describes the decay rate of the mean biomass contribution of the ith population to the community according to $\mu_i = \mu_1 e^{-a(i-1)}$, where μ_i is the mean contribution of the ith most abundant population (see Appendix for calculation).

‡ Rotifer biomass estimates were not available during the years 1986, 1992, and 1993.

elaborated by Scargle (1982). The Lomb-Scargle algorithm differs from traditional spectral analysis in that it considers the distribution of sampling events in time when evaluating the periodogram.

Using evenly spaced data one can estimate the spectrum up to the Nyquist frequency $f = (2\Delta t)^{-1}$ where Δt is the sampling interval (Chatfield 2004). For unevenly sampled data, the sampling interval is not consistent, and theoretically, the periodogram can be determined up to $(2\Delta t_{\text{min}})^{-1}$. However, estimates above the mean Nyquist frequency $(2\Delta t_{\text{mean}})^{-1}$ can be biased due to aliasing and low power, since there may be very few samples at the shortest sampling intervals. We estimated the Lomb-Scargle periodogram $\hat{P}(f)$ up to the mean Nyquist frequency $(2\Delta t_{\text{mean}})^{-1}$ using the algorithm supplied by Press et al. (2001). The Lomb-Scargle periodogram $\hat{P}(f)$ represents the reduction in the sum-of-squares of $X(t_j)$ that would result from removal or "detrending" of an oscillation with frequency f. The spectrum $\hat{S}(f)$ is then generated by smoothing the periodogram using a Bartlett window (tapered moving average) of breadth $M = 6$ (see Chatfield 2004):

$$\hat{S}(f) = \frac{1}{2M+1}\sum_{j=-M}^{M} P(f_j)\left(1 - \frac{|j|}{M}\right). \tag{2}$$

We estimated the spectrum for each of the 36 phytoplankton, 25 ciliate, 21 rotifer, and seven crustacean populations in Lake Constance ($\hat{S}_i$) and for the four aggregate communities ($\hat{S}_{\text{C}}$). Prior to estimation of the spectrum, we log-transformed the data to make them better approximate a normal distribution on the proportional scale and to account for the mean–variance scaling relationship (e.g., McArdle et al. 1990). In the rare populations, biomass frequently drops below the threshold of detection resulting in an observed "zero" biomass in the raw data. Commonly, this is overcome by adding a constant to each data point prior to transformation (e.g., Rusak et al. 2002) but this has been shown to underestimate the true variance (McArdle et al. 1990). Since the Lomb-Scargle algorithm is effective down to very low sample sizes (Horne and Baliunas 1986), we employ in our analysis only the sampling dates on which positive biomass was recorded. Further, any error introduced by zero omission has a negligible impact on the results because rare species (those with the most zeros) are only weakly represented in the weighted mean population spectrum (see *Determination of stability-influencing mechanisms*).

To supplement the frequency-domain information, we estimated the phases of periodic components in the population-level data at two particular frequencies ($f = 1$ and 2 cycles/yr; the reason for this choice is made clear in *Results*). As in Vasseur et al. (2005), harmonic least-squares regression was used to estimate the mean, amplitude, and phase of the dominant periodic component ($f = 1$ cycle/yr). This signal was then removed from the time-series by detrending (see Chatfield 2004) and the process was repeated for the subsequent periodic component ($f = 2$ cycles/yr).

Determination of stability-influencing mechanisms

As in the previously described example, the presence of synchronous and compensatory population dynamics can be inferred by comparing the community spectrum to the mean population spectrum. However, unlike the "idealized" example, biomass is not evenly distributed among populations; on any given sampling date, five or fewer populations commonly contribute more than 80% of the community biomass (see Appendix). When a large fraction of community biomass is derived from a few dominant populations, community variability is most sensitive to the dynamic relationships (synchronous, compensatory, or independent) between these dominant populations. Therefore, a more reliable mean of the individual population spectra (which do not reflect the dominance or rarity of their biomass in the community) is obtained by weighting them by their contribution to community biomass. We compute this weighted geometric mean population spectrum, $\hat{S}_{\text{P}}(f)$, for each of the four plankton communities as

$$\hat{S}_{\text{P}}(f) = \sum_{i=1}^{n}[w_i \log \hat{S}_i(f)] \tag{3}$$

where

$$\sum_{i=1}^{n} w_i = 1.$$

and where the weights (w_i) represent the mean relative contribution of each population i to the total community biomass and n is the number of populations in the community (see Table 1). We herein refer to this as the mean population spectrum. The 95% confidence intervals for the mean population spectrum are determined using the formula for the variance of a geometric weighted mean:

$$\hat{S}_{\mathrm{P}}(f) \pm t_{\alpha/2,n-1}\frac{1}{n}\sqrt{\frac{1}{1-\sum_{i=1}^{n} w_i^2}\sum_{i=1}^{n}\left\{w_i[\log\hat{S}_i(f)-\hat{S}_{\mathrm{P}}(f)]^2\right\}}. \tag{4}$$

To aid in highlighting the temporal scales at which synchronous and compensatory dynamics impact on community variability is important, we calculated two frequency-resolved measures of the coherence between the community and mean population spectra. The difference in explained variance,

$$\Delta\mathrm{EV} = \hat{S}_{\mathrm{C}}(f) - \hat{S}_{\mathrm{P}}(f) \tag{5}$$

describes the absolute change in explained variance from the mean population to the community level. Under ideal conditions (even biomass distribution amongst populations and mean/variance rescaling exponent $z = 2$) ΔEV will always be zero or less (where zero indicates perfect population synchrony), however, positive values are possible when biomass distributions are uneven and z values deviate from two. Large absolute changes in ΔEV occur at scales which are extremely important for relationships driving community-level variability. The second measure, the explained variance ratio,

$$\mathrm{EVR} = \hat{S}_{\mathrm{C}}(f)/\hat{S}_{\mathrm{P}}(f) \tag{6}$$

describes the relative change in explained variance from the mean population to the community level. Under ideal conditions, the EVR has a maximum value of one when population dynamics are perfectly synchronous and a minimum value of zero when population dynamics are perfectly compensatory. The value of EVR which marks the transition from synchrony to compensation ($\mathrm{EVR_T}$) occurs when populations vary independently. We calculate transition values ($\mathrm{EVR_T}$) for the four communities according to

$$\mathrm{EVR_T} = \frac{(1-e^{-a})(1+e^{-an})}{(1+e^{-a})(1-e^{-an})} \tag{7}$$

which is based upon richness (n) and an inverse measure of evenness (a; see Table 1 for parameter values and Appendix for the derivation of Eq. 7). The $\mathrm{EVR_T}$ vary between 0.14 and 0.34, demonstrating that portfolio effects can be responsible for as little as a threefold to as much as a sevenfold reduction in community variance in the Lake Constance plankton (Table 2). We use these thresholds to determine at which frequencies population dynamics are synchronous ($\mathrm{EVR} > \mathrm{EVR_T}$) and at which frequencies population dynamics are compensatory ($\mathrm{EVR} < \mathrm{EVR_T}$).

RESULTS

Fig. 3 shows the results of the spectral analysis for each of the four plankton communities (phytoplankton, ciliates, rotifers, and crustaceans; see Plate 1) in Lake Constance. In each figure panel, the individual population spectra, the mean population spectrum and its 95% confidence limits, and the community spectrum are shown. At each frequency f the explained variance $\hat{S}(f)$ is proportional to the reduction in the sum of squares that is achieved by removing a periodic component with frequency f from the time series. The area under the spectrum is proportional to the temporal variance; so spectra that cover more area describe populations (or communities) with greater temporal variability. We show explained variance on a logarithmic scale to account for the large distribution of values.

It is evident from the peaks in Fig. 3, that relatively few frequencies explain a large portion of the temporal variance in the Lake Constance plankton (these peaks are especially large given the logarithmic scale of the y-axis in Fig. 3). The frequency 1 cycle/yr, which corresponds to variability imposed by annual dynamics, explains the largest amount of temporal variability in the mean population and community spectra for each of the four plankton communities. In phytoplankton, ciliates, and rotifers, four subordinate frequencies, occurring at the harmonic intervals 2, 3, 4, and 5 cycles/yr, also explain large amounts of temporal variability. In crustaceans, the latter frequency (5 cycles/yr) is not expressed. Frequencies above 6 cycles/yr exhibit relatively little explanatory power and vary only slightly over this range (recall the logarithmic scale of explained variance on Fig. 3). There is a trend toward increasing explanatory power at the lowest frequencies (0.05 cycles/yr) in the mean population spectra and, to a lesser extent, the community spectra for phytoplankton, ciliates, and crustaceans. We do not show the spectra for rotifers at frequencies below 0.3 cycles/yr because the longest period of continuous measure of rotifers is only six years (see Table 1). Herein we refer to the five frequencies (1, 2, 3, 4, and 5 cycles/yr) as the fundamental frequencies (f_1, f_2, f_3, f_4, f_5), given that they explain the largest amounts of temporal variance in the Lake Constance plankton.

While the mean population spectrum demonstrates the contribution of each frequency to the temporal variability of the "mean" population, it is worthwhile to investigate the coherence between the spectra of individual populations and the mean population spectrum at the fundamental frequencies. In phytoplankton, crustaceans, and ciliates (to a lesser extent), there is strong coherence between populations and the mean population spectrum at the fundamental frequencies; the majority of populations share these fundamental frequencies. In rotifers, there are large differences among the population spectra at these fundamental frequencies, indicating that they are not shared by all populations. However, the narrow breadth of the confidence limits

TABLE 2. Aggregate measures of temporal variability and characteristic measures of the relationship between population and community variability in the four plankton communities.

Community	Mean population variance (σ_P^2)†	Community variance (σ_C^2)	Mean–variance scaling exponent (z)‡	Explained variance ratio threshold (EVR_T)§
Phytoplankton	0.61	0.22	1.86 ± 0.015	0.16
Ciliates	0.32	0.24	1.73 ± 0.025	0.14
Rotifers	0.99	1.06	1.80 ± 0.02	0.25
Crustaceans	0.58	0.21	1.80 ± 0.05	0.34

Note: Boldface type denotes compensatory dynamics within the community ($EVR < EVR_T$).

† Calculated from the spectrum integral: $\int \hat{S}_P(f)df$.

‡ Calculated by regressing the annual log population variance against annual log mean biomass.

§ Calculated considering the influence of community richness and evenness. See the Appendix for the derivation.

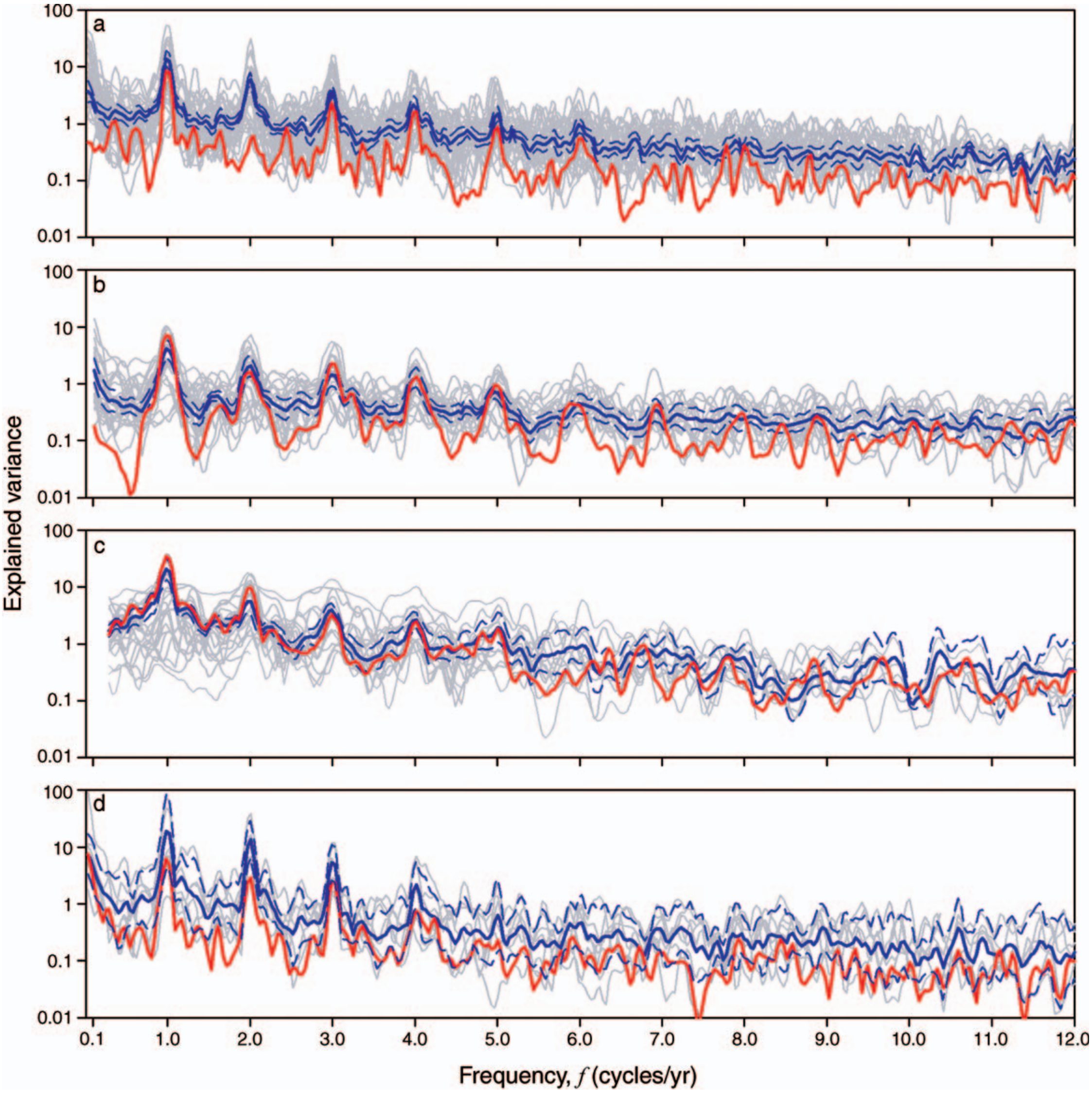

FIG. 3. Population and community spectra of the four Lake Constance plankton communities: (a) phytoplankton, (b) ciliates, (c) rotifers, and (d) crustaceans. The solid blue line is the weighted geometric mean population spectrum, and the dashed blue lines show its 95% confidence interval. The solid red line is the spectrum of community biomass, and the light gray lines in the background show the spectra of each individual population. Frequency is shown in cycles per year to ease interpretation. The original calculations were done in cycles per day. Note the y-axis log scale.

TABLE 2. Extended.

Integrated explained variance ratio $\left(\frac{\sigma_C^2}{\sigma_P^2}\right)$	Explained variance ratio at f_1	Explained variance ratio at f_2
0.36	0.632	**0.091**
0.75	1.81	0.778
1.07	1.71	1.76
0.35	**0.281**	**0.214**

for the mean population spectrum indicates that the fundamental frequencies are shared, at least, by the populations that dominate the rotifer biomass. The confidence limits are generally broader for crustaceans than for the other plankton groups due to the relatively low number of populations contributing to the crustacean community. The observed increase in breadth of the confidence limits at high frequencies (mainly in rotifers and ciliates) is partly due to a lack of information for some populations with low mean Nyquist frequencies (resulting in a smaller N). This effect is prominent in rotifers since their life history often contains non-planktonic stages. Since most ciliated morphotypes are present year-round in the plankton (U. Gaedke, *unpublished manuscript*), the increase in breadth of their confidence limits is more likely due to independent population dynamics at these scales.

From the model communities 1 and 2, it is evident that the coherence between population spectra and the community spectrum can be used to infer whether synchronous or compensatory dynamics are common among populations. For each plankton community we compare the mean population spectrum to the community spectrum. Since the fundamental frequencies explain a large portion of the temporal variability, coherence (or non-coherence) between the mean population and community spectra at these frequencies is much more important to temporal variability than coherence (or non-coherence) at frequencies which explain a lesser portion of the temporal variability. With only one clearly visible exception, f_2 in phytoplankton, there is generally strong coherence between the mean population and community spectra at the fundamental frequencies in all four plankton communities (see Fig. 3). This suggests that synchronous dynamics are common among the dominant populations at these frequencies. For rotifers, this coherence holds at all frequencies (Fig. 3c). For phytoplankton, ciliates, and crustaceans, there is a breakdown in coherence between the community and mean population spectra (e.g., the community spectrum explains less variance) between the fundamental frequencies, at all frequencies greater than approximately 6 cycles/yr, and below 1 cycle/yr. However, it should be noted that the absolute difference between the two spectra is magnified at lower values of explained variance due to the logarithmic scale of the y-axis.

To improve the visibility of absolute changes in explained variance between the mean population and community spectra we plot their difference (ΔEV) on a linear scale for each of the four plankton communities (Fig. 4). In the same figure, we show the explained variance ratio (EVR) and the thresholds ($\mathrm{EVR_T}$) for each community at the fundamental frequencies. Recall

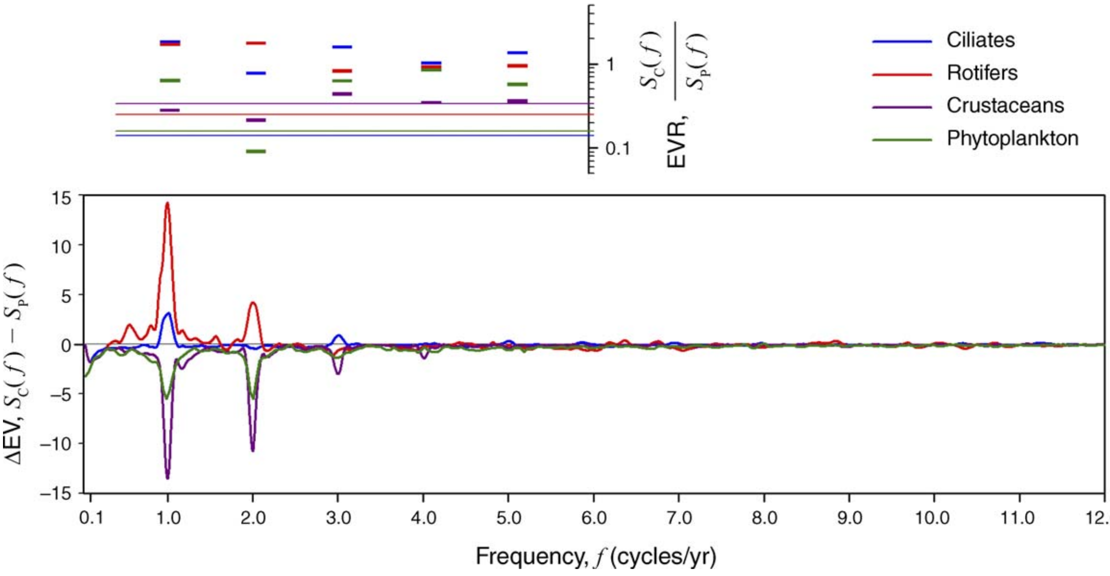

FIG. 4. The change in explained variance (ΔEV) from the mean population to the community for phytoplankton (green), ciliates (blue), rotifers (red), and crustaceans (violet). The explained variance ratio (EVR) is shown for the fundamental frequencies that are responsible for the largest change in variance in each of the communities (inset panel). The reference lines are the thresholds separating synchronous from compensatory dynamics calculated independently for each community based upon richness and evenness (see Appendix).

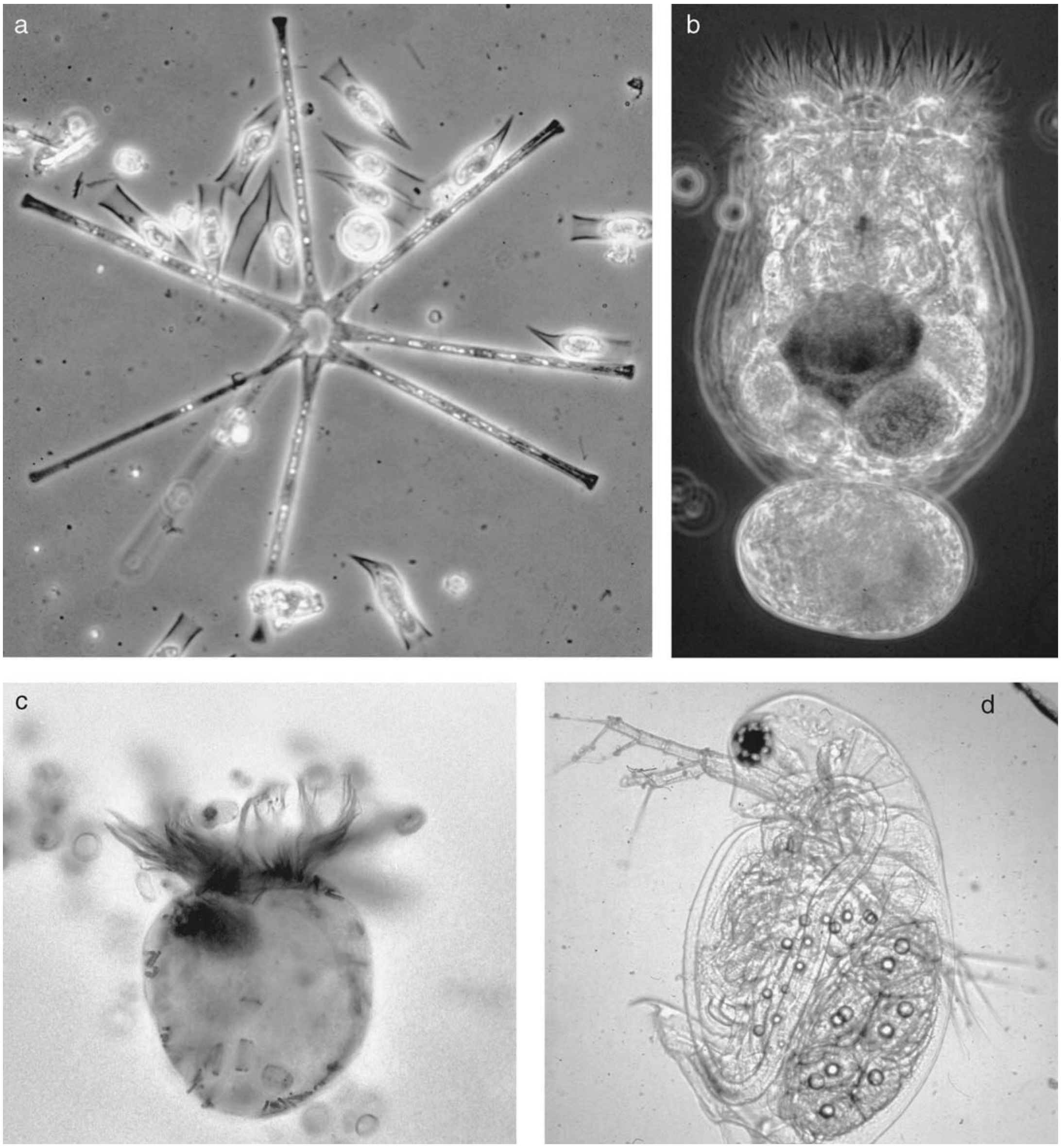

PLATE 1. Representative organisms from the four plankton communities: (a) phytoplankton (*Asterionella formosa* and *Dinobryon divergens*); (b) ciliates (*Strobilidium humile*) with some small phytoplankton (*Stephanodiscus hantzschii*, a centric diatom) in the background and ingested; (c) rotifers (*Brachionus* sp.); and (d) crustaceans (*Daphnia galeata longispina*, with eggs under the carapace). Photo credits: images (a), (c), and (d) by U. Gaedke; image (b) by Helga Müller.

that the threshold indicates the predicted value of EVR for independent dynamics, and when $\mathrm{EVR} < \mathrm{EVR_T}$ population dynamics are thus compensatory (and synchronous for the alternative case). Population dynamics at the first three fundamental frequencies have the largest impact on the difference in explained variance. For phytoplankton and crustaceans, population dynamics at f_1 and f_2 generate large negative values of ΔEV. In phytoplankton, the EVR indicates that the population dynamics at f_1 are synchronous, while the reduction at f_2 arises from dynamics that are compensatory (Fig. 4, Table 2). Here, the importance of considering the absolute (ΔEV) and relative (EVR) changes is exemplified; a similar absolute change in explained variance occurs at these two frequencies despite different dynamic relationships between populations. At f_1, the substantial negative value of ΔEV arises because slight deviations from perfect synchrony (e.g., when $\mathrm{EVR} = 1$) are amplified by the large amount of explained variance in the mean population spectrum; whereas at f_2 the ΔEV is amplified by compensatory dynamics. For crustaceans the EVR is less than the threshold ($\mathrm{EVR_T}$) at f_1 and f_2 (Table 2) indicating that compensatory dynamics occur at these frequencies.

Positive values of ΔEV are observed at f_1 and f_3 (for ciliates) and f_1 and f_2 (for rotifers) due to strong population synchrony (EVR $\gg$ EVR$_T$) at these fundamental frequencies. Despite evidence for reductions in the explained variance at other frequencies only the first three fundamental frequencies have a noticeable impact on community variance (Fig. 4) since the remaining frequencies explain only small amounts of variance (see Fig. 3).

If we integrate the spectra in Fig. 3, the temporal variance of the process is returned, thus we can compare the variance of the mean population and the variance of the community within and between the four plankton communities. Rotifer populations exhibit the largest variance at the population level, followed by phytoplankton, crustaceans, and ciliates (Table 2). At the community level rotifers again have by far the largest variance followed by ciliates, phytoplankton, and crustaceans (Table 2). Accordingly, the two communities which exhibit compensatory dynamics have the largest reduction in variance when aggregating populations into communities; the crustacean and phytoplankton communities exhibit only 35% and 36% as much variance as their mean populations, respectively. Despite the observed positive values of ΔEV for ciliates the community exhibits only 76% as much variance as the mean population, indicating that frequencies outside the fundamental ones collectively have an important impact on community variance. The rotifer community exhibits 107% as much variance as the mean population attesting to the strength of synchrony among the dominant populations at all frequencies in this community.

To demonstrate how synchronous and compensatory dynamics are achieved in the four communities, we plot the phases of each population at the first two fundamental frequencies (Fig. 5). These plots are polar plots, with phase measured in radians, to reflect the fact that a population whose phase is slightly greater than zero is closely associated (in synchrony) with one whose phase is slightly less than 2π. The two examples presented in the *Methods* section, demonstrate how synchrony and compensation arise from the distribution of phases; perfect synchrony (shown at f_1) requires an exact overlay of phases whilst perfect compensation (shown at f_2) requires a consistent difference between phases or clusters of phases (Fig. 5). At f_1, the strong synchrony predicted for ciliates and rotifers by the spectral method (Fig. 4, Table 2) is clearly visible as a clustering of phases into the second quarter of the phase domain (i.e., most species have their maximum around spring/early summer). Synchrony in phytoplankton, which is weaker than in ciliates and rotifers, is visible as a weaker clustering of phases, covering the first half of the phase domain (i.e., species peak either in spring or summer but not in autumn or winter). The most prevalent compensatory dynamic, responsible for a 10-fold variance reduction in phytoplankton at f_2 (Fig. 4, Table 2), arises from a distribution of phases approaching uniformity across the domain (similar to our exemplary model 2; Fig. 5). In crustaceans, a different pattern is responsible for compensatory dynamics at f_1. At f_1, the phases of crustaceans form two distinct clusters; within each cluster the dynamics are synchronous, but compensatory dynamics ultimately arise as a consequence of the phase difference between the clusters (Fig. 5). When interpreting the results for ciliates, rotifers, and crustaceans at f_2 particular attention must be paid by to the relative importance of each population. Synchrony results from the rather uniform distribution of phases in ciliates and from the two clusters in rotifers at f_2 because the most important morphotypes remain restricted to a small fraction of the phase domain (Fig. 5). In crustaceans, at f_2 the origin of compensatory dynamics is less clear; the phase distribution is uniform over only half the phase domain (Fig. 5). While not as strong as the compensation arising from a fully uniform distribution of phases (*cf.* phytoplankton at f_2; Fig. 5) there is enough difference among phases to generate compensatory dynamics. With the exception of f_2 in crustaceans, the patterns of synchrony and compensation found at f_1 and f_2 by comparing the community and mean population spectra (Table 2) correspond quite well to a visual inspection of the patterns in Fig. 5.

DISCUSSION

Using two examples we have shown how frequency-dependent synchronous and/or compensatory dynamics can be detected by comparing the population and community spectra and we have applied this method to data from four plankton communities in Lake Constance. Our results show that the fundamental frequencies, f_1, f_2, f_3, f_4, and f_5, are extremely important for population and community variability. Synchronous dynamics predominate among the dominant populations in each of the four plankton communities in Lake Constance. However, compensatory population dynamics are evident at f_2 in phytoplankton and at f_1 and f_2 in crustaceans. Compensatory population dynamics largely reduce community variance relative to population variance in phytoplankton and crustaceans while synchronous dynamics drive only small reductions (in ciliates) and increases (in rotifers; Table 2). Despite the 10-fold reduction in community relative to population variability that occurs as a consequence of compensatory dynamics in phytoplankton at f_2, the same measure integrated across all frequencies (the ratio of temporal variances) depicts only a three-fold reduction (Table 2) attesting to the utility of this scale-resolving method for unmasking scale-dependent population dynamics.

The variance of aggregates (of species, populations, communities, etc.) has tended to be less than the variance of their members in a variety of studies, although most focus on plants and few span multiple trophic levels (for a review, see Hooper et al. 2005). A recent study of crustacean variability in 22 unmanipulated northern temperate lakes found that the variance

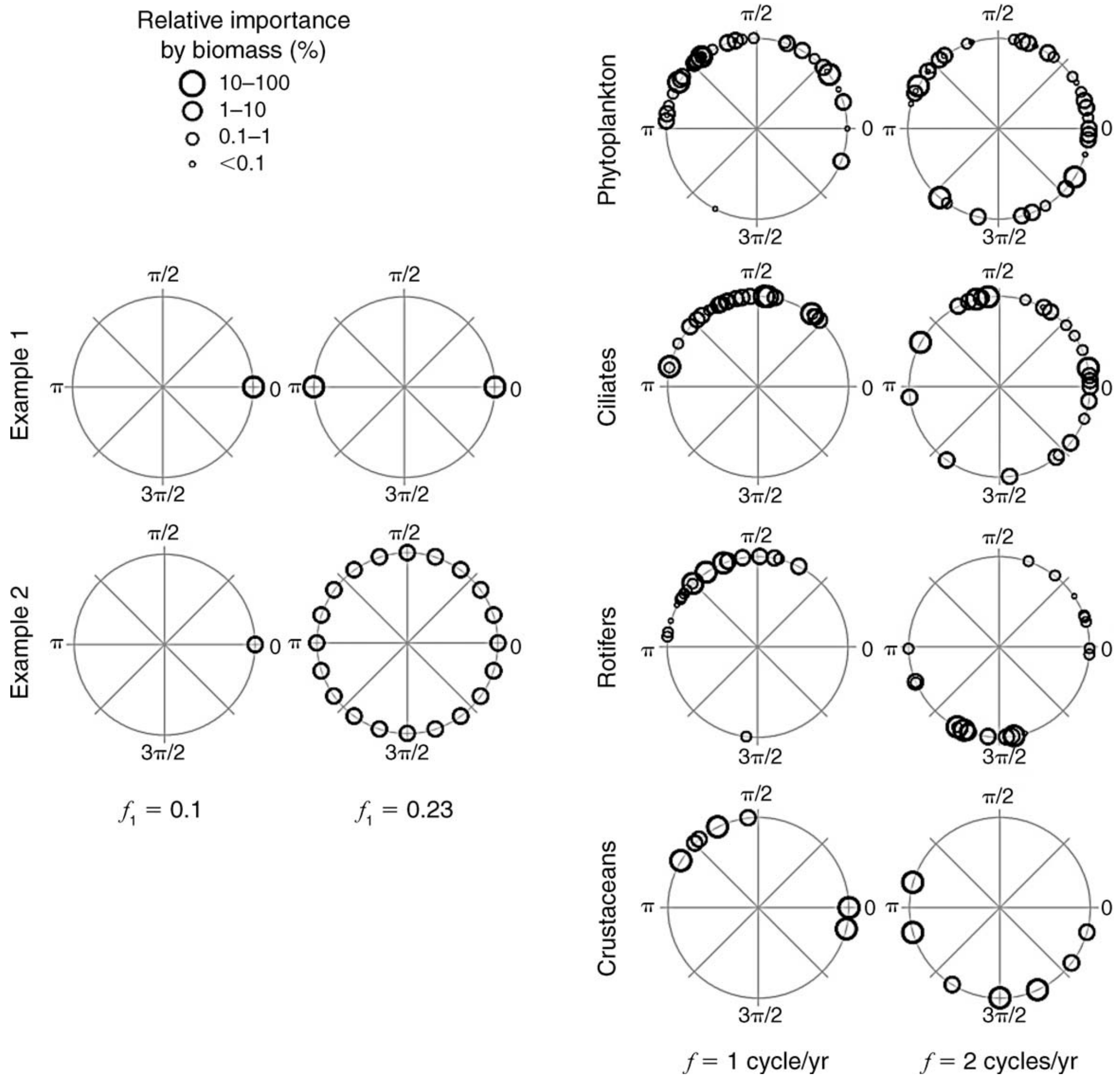

FIG. 5. The phases of periodic components at the first two fundamental frequencies (f_1 and f_2) for all populations in the two example communities (cf. Figs. 1 and 2) and in each of the four plankton communities. Phases are plotted as angular coordinates (in radians) on polar plots with a fixed radius. Each ring represents the phase of a single population, and the size of the ring is proportional to its relative contribution to the community biomass (the same set of weights governing Eq. 3). For the example, communities 1 and 2, all phases are equal at f_1 and thus are directly overlaid on the figure. Phases were estimated using least-squares harmonic regression.

of total crustacean biomass was on average 38% of that of the crustacean functional groups (using log-transformed data [Rusak et al. 2002]). Similar work has been conducted on the plankton of Lake Constance using a different measure of variability than that employed here; Gaedke et al. (1996) showed that the CV of phytoplankton, ciliate, rotifer, and crustacean biomass decreased when populations were aggregated into communities (reductions to 35%, 41%, 52%, and 64% respectively). In oligotrophic Königssee, similar respective reductions in the CVs to 25%, 30%, 40%, and 39% occurred (Gaedke et al. 1996). Our results for ciliates and rotifers differ from these earlier studies since we employ a different metric, log-transformed data, and we employ a weighted mean of all populations to determine the mean population variance whereas Gaedke et al. (1996) used an unweighted mean of only those morphotypes which were determined to the species level.

In Lake Constance, previous attempts at implicating compensatory dynamics in the observed reduction from population to community variance have proven inconclusive. The traditional variance ratio (the ratio of community variance to the summed population variances; e.g., Schluter [1984]) predicts that populations are synchronous or independently fluctuating within all four plankton communities in Lake Constance (over the entire monitoring period and during individual seasons; U. Gaedke, *unpublished manuscript*). However, the variance ratio neither accounts for the lognormal distribution of plankton abundance, which biases the results toward high-abundance periods (although root transforms have been used in U. Gaedke [*unpublished manuscript*]), nor does it resolve the confounding problem introduced by temporal scale. The results of this study show that when temporal scale is resolved, compensatory dynamics can be observed and their effects can be quantified where traditional measures have previously failed.

The vast majority of experimental studies which have manipulated richness or diversity have generated results consistent with portfolio effects rather than compensatory dynamics (e.g., Petchey et al. 2002, Steiner et al. 2005). Quantifying the influence of the portfolio effect is arduous in natural data, given that it is strongly inhibited by a lack of evenness (Cottingham et al. 2001) and confounded by the mean-scaling exponent, by the heterogeneity in population productivity, overyielding, and by correlated responses to the environment (Doak et al. 1998, Lhomme and Winkel 2002). Our threshold values ($\mathrm{EVR_T}$) used to distinguish compensatory from synchronous population dynamics incorporate the influence of both the richness and evenness of the four communities (see Appendix) but do not account for the impact of the remaining factors. One of the assumptions required when comparing variances derived from log-transformed biomass is that the mean-scaling exponent (z) equals 2. While we have demonstrated some deviation of these values in our data (see Table 2) they all deviate in the direction which diminishes the portfolio effect (Tilman et al. 1998, Cottingham et al. 2001). While we cannot quantify the influence of other factors such as heterogeneity in productivity and/or overyielding in our data, the assumptions made during the threshold calculations (see Appendix) reduce the possibility of falsely detecting compensatory dynamics.

Although the reductions in explained variance which we attribute to frequency-dependent compensatory dynamics are larger than those that would be expected from the Portfolio effect alone, the total reductions in variance (integrated EVR; Table 2) suggest that synchronous dynamics are predominant in all but the crustaceans, where population dynamics appear independent. The total reduction from population to community variability in phytoplankton, ciliates, and crustaceans is largely in agreement with the level of population synchrony shown in U. Gaedke (*unpublished manuscript*). However, for rotifers, Gaedke (*unpublished manuscript*) detected less synchrony than within ciliates, while this study finds rotifers the most synchronized of the four plankton communities. We suspect that this difference arises from synchronization of the three dominant rotifer morphotypes, which contribute 71% of the total weight in the mean population spectrum. This difference demonstrates that more effort is required to obtain a meaningful measure of synchrony in communities with low evenness and high fluctuations in population biomass.

Compensatory dynamics have been observed, and to some degree quantified, in only a small number of natural and experimental systems (for a review see Micheli et al. 1999, Fischer et al. 2001, Keitt and Fischer 2006) despite the large effort that has gone into detecting richness–variability relationships (Loreau et al. 2002). Of those studies detecting compensatory dynamics, most have expressed a requirement for both biotic and abiotic regulatory factors (Micheli et al. 1999). Compensatory dynamics have been previously quantified in the Lake Constance phytoplankton and attributed to the interaction between edible and less-edible functional groups, which is mediated by competition for nutrients and grazing by predators during the growing season (Vasseur et al. 2005). However, that study identified only a two- to threefold reduction in community relative to population variability at f_2, in distinct contrast to the 10-fold reduction detected here. This suggests that important compensatory processes must occur within both the edible and less-edible functional groups in addition to those previously shown to exist between them. The uniformity of the phase plot at f_2 shows no clear clustering of "functional groups" (Fig. 5) enforcing that population-level dynamics are as or more important than relationships between functional groups.

Crustaceans exhibit reductions in community relative to population variance which are attributable to compensation at the first two fundamental frequencies. The crustacean community in Lake Constance is dominated by predominantly herbivorous filter-feeding cladocerans such as daphnids, and by raptorial feeding, omnivorous calanoid and cyclopoid copepods. These two copepods are set distinctly apart from the cladocerans in the phase plots at f_1 and at f_2 (Fig. 5) which reflects the different seasonal dynamics of the two groups of crustaceans (Straile and Geller 1998) and influences compensatory dynamics at both frequencies. It is already well known that the dynamics of cladocerans are strongly tied to those of edible phytoplankton, on which they feed predominantly, while for copepods the respective pattern holds for larger (less-edible) phytoplankton (Sommer et al. 2003, Huber and Gaedke 2006). The existence of these feeding links suggests that compensatory dynamics in crustaceans, in particular at f_2, is strongly tied to compensatory dynamics in phytoplankton at the same temporal scale. In Little Rock Lake (Wisconsin, USA) scale-resolving methods have demonstrated synchrony between two species of *Daphnia* and compensation between two species of carnivorous copepods at the seasonal scale, and opposite patterns of synchrony and compensation at longer time scales due to experimental acidification (Keitt and Fischer 2006). While there is little doubt that compensation is important for ecosystem function, there is still much to be learned by better understanding how environmental and biotic factors drive synchrony and compensation in these freshwater systems and elsewhere.

The importance of synchronous or compensatory dynamics in our scale-resolved analysis depends largely on the magnitude of explained population-level variance at the scales where synchrony or compensation occurs; larger magnitudes have an increased potential to significantly alter the community-level variability. What remains unclear from our results is which environmental or biotic processes cause populations and communities to vary more or less at certain frequencies. The general trend of having larger amounts of explained variance at low frequencies has been observed in many populations (e.g., Pimm and Redfearn 1988, Inchausti and Halley 2002). This relationship often follows a power-law of the form $1/f^{\beta}$ where β takes on a value greater than zero. All of the population and community spectra calculated in this analysis adhere to this relationship. In Lake Constance, the increase in spectral power at temporal scales above one year may represent the response to substantial re-oligotrophication (see Gaedke 1998). The peak in explained variance at f_1 originates from the seasonal succession of events that occur in temperate lakes (Sommer et al. 1986), but the origin of the peaks at higher fundamental frequencies is less clear. Laboratory experiments have established that predator–prey or stage-structured population cycles commonly occur in cladocerans and phytoplankton at sub-annual frequencies (McCauley et al. 1996, Grover et al. 2000) and fluctuations of phytoplankton, crustaceans, and ciliates during the growing season in Lake Constance appear consistent with this (Gaedke et al. 2002). However, determining the exact origins of periodic variability requires a more thorough analysis than can be devoted here (e.g., Kendall et al. 1999). From a statistical, rather than ecological, perspective, "spectral leakage" can introduce artifactual power into the harmonic frequencies of a dominant cycle (Horne and Baliunas 1986, Chatfield 2004). However, the harmonic frequencies in phytoplankton have proven significant even when the effects of leakage are accounted for (Vasseur et al. 2005) and we expect this result to hold for the remaining plankton communities. Peaks may also arise at harmonic frequencies if the annual dynamics are best described by a waveform that is non-sinusoidal (e.g., triangular). Yet, the highly different dynamical relationships found at f_1 and f_2 suggests that the peaks have interpretations beyond those of pure artifact. While the origin of the peaks at the higher fundamental frequencies is an issue deserving further investigation, the relationships between the mean population and community spectra at these and other frequencies are a robust description of the population dynamic patterns, regardless of their origin (environmental, biological, or artifactual).

Levin (1992) stressed the need for analytical methods capable of quantifying variability patterns in space and time, and we have shown here how one such method can highlight temporal scales at which population dynamics are predominantly important for community variability. The method employed here, while teasing apart the effects of dynamics at different temporal scales, makes maximal use of the data, incorporating all sampling events despite the temporal variability in sampling effort. In addition, the aggregate variability estimates that are gained by integrating the spectrum provide a measure of the temporal variance that is not biased by the sampling protocol. The method also accounts for the uneven distribution of biomass among populations; the contribution of each population to the mean population spectrum relies on its relative contribution to the total community biomass. This is a reliable approach for obtaining dynamical patterns since the relationships between dominant species, be them compensatory or synchronous, influence the community variability more strongly than the relationships between rare species. Future application of this, and other scale-resolving methods, to a variety of systems, both terrestrial and marine, promises to make better use of available data by unmasking previously obscured dynamic patterns among populations or functional groups. Determining the mechanistic foundation upon which compensatory and synchronous dynamics are driven will ultimately lead to a better understanding of ecosystem stability.

ACKNOWLEDGMENTS

Data acquisition was partially performed within the Special Collaborative Program (SFB) 248 "Cycling of Matter in Lake Constance" supported by Deutsche Forschungsgemeinschaft. Conversations with H. Cyr, K. Cottenie, and K. McCann aided our interpretation of the results. J. Fox, G. Fussmann, F. Guichard, V. Huber, and K. Trzcinski provided valuable feedback on the manuscript. We thank Helga Müller for providing the ciliate photograph.

LITERATURE CITED

Chatfield, C. 2004. The analysis of time series: an introduction. CRC Press, Boca Raton, Florida, USA.

Cottingham, K. L., B. L. Brown, and J. T. Lennon. 2001. Biodiversity may regulate the temporal variability of ecological systems. Ecology Letters 4:72–85.

Doak, D. F., D. Bigger, E. K. Harding, M. A. Marvier, R. E. O'Malley, and D. Thomson. 1998. The statistical inevitability of stability–diversity relationships in community ecology. American Naturalist 151:264–276.

Fischer, J. M., T. M. Frost, and A. R. Ives. 2001. Compensatory dynamics in zooplankton community responses to acidification: measurement and mechanisms. Ecological Applications 11:1060–1072.

Gaedke, U. 1998. Functional and taxonomical properties of the phytoplankton community: interannual variability and response to re-oligotrophication. Archiv für Hydrobiologie, Special Issues, Advances in Limnology 53:119–141.

Gaedke, U., T. Barthelmess, and D. Straile. 1996. Temporal variability of standing stocks of individual species, communities, and the entire plankton in two lakes of different trophic state: empirical evidence for hierarchy theory and emergent properties? Senckenbergiana Maritima 27:169–177.

Gaedke, U., S. Hochstädter, and D. Straile. 2002. Interplay between energy limitation and nutritional deficiency: empirical data and food web models. Ecological Monographs 72: 251–270.

Grover, J. P., D. McKee, S. Young, H. C. J. Godfray, and P. Turchin. 2000. Periodic dynamics in *Daphnia* populations: biological interactions and external forcing. Ecology 81: 2781–2798.

Hooper, D. U., et al. 2005. Effects of biodiversity on ecosystem functioning: a consensus of current knowledge. Ecological Monographs 75:3–35.

Horne, J. H., and S. L. Baliunas. 1986. A prescription for period analysis of unevenly sampled time series. Astrophysical Journal 302:757–763.

Huber, V. E. C., and U. Gaedke. 2006. The role of predation for seasonal variability patterns among phytoplankton and ciliates. Oikos 114:265–276.

Inchausti, P., and J. Halley. 2002. The long-term temporal variability and spectral colour of animal populations. Evolutionary Ecology Research 4:1033–1048.

Keitt, T. H., and J. Fischer. 2006. Detection of scale-specific community dynamics using wavelets. Ecology 87:2895–2904.

Keitt, T. H., and D. L. Urban. 2005. Scale-specific inference using wavelets. Ecology 86:2497–2504.

Kendall, B. E., C. L. Briggs, W. M. Murdoch, P. Turchin, S. P. Ellner, E. McCauley, R. M. Nisbet, and S. N. Wood. 1999. Why do populations cycle? A synthesis of statistical and mechanistic modeling approaches. Ecology 80:1789–1805.

Klug, J. L., J. M. Fischer, A. R. Ives, and B. Dennis. 2000. Compensatory dynamics in planktonic community responses to pH perturbations. Ecology 81:387–398.

Levin, S. A. 1992. The problem of pattern and scale in ecology. Ecology 73:1943–1967.

Lhomme, J. P., and T. Winkel. 2002. Diversity–stability relationships in community ecology: re-examination of the portfolio effect. Theoretical Population Biology 62:271–279.

Lomb, N. R. 1976. Least-squares frequency analysis of unequally spaced data. Astrophysics and Space Science 39: 447–462.

Loreau, M., S. Naeem, and P. Inchausti, editors. 2002. Biodiversity and ecosystem functioning: synthesis and perspectives. Oxford University Press, Oxford, UK.

McArdle, B. H., K. J. Gaston, and J. H. Lawton. 1990. Variation in the size of animal populations: patterns, problems and artifacts. Journal of Animal Ecology 59:439–454.

McCann, K. S. 2000. The diversity–stability debate. Nature 405:228–233.

McCauley, E., R. M. Nisbet, A. M. Deroos, W. W. Murdoch, and W. S. C. Gurney. 1996. Structured population models of herbivorous zooplankton. Ecological Monographs 66:479–501.

Micheli, F., K. L. Cottingham, J. Bascompte, O. N. Bjørnstad, G. L. Eckert, J. M. Fischer, T. H. Keitt, B. E. Kendall, J. L. Klug, and J. A. Rusak. 1999. The dual nature of community variability. Oikos 85:161–169.

Müller, H., A. Schöne, R. M. Pinto-Coelho, A. Schweizer, and T. Weisse. 1991. Seasonal succession of ciliates in Lake Constance. Microbial Ecology 21:119–138.

Murdoch, W. W., and A. Stewart-Oaten. 1989. Aggregation by parasitoids and predators: effects on equilibrium and stability. American Naturalist 134:288–310.

Petchey, O. L., T. Casey, L. Jiang, P. T. McPhearson, and J. Price. 2002. Species richness, environmental fluctuations, and temporal change in total community biomass. Oikos 99:231–240.

Pimm, S. L., and A. Redfearn. 1988. The variability of population densities. Nature 334:613–614.

Press, W. H., S. A. Teukolsky, W. T. Vetterling, and B. T. Flannery. 2001. Numerical recipes in Fortran 77: the art of scientific computing. Second edition. Volume 1 of Fortran numerical recipes. Cambridge University Press, Cambridge, UK.

Rusak, J. A., N. D. Yan, K. M. Somers, K. L. Cottingham, F. Micheli, S. R. Carpenter, T. M. Frost, M. J. Paterson, and D. J. McQueen. 2002. Temporal, spatial, and taxonomic patterns of crustacean zooplankton variability in unmanipulated north-temperate lakes. Limnology and Oceanography 47:613–625.

Scargle, J. D. 1982. Studies in astronomical time series analysis. II. Statistical aspects of spectral analysis of unequally spaced data. Astrophysical Journal 263:835–853.

Schluter, D. 1984. A variance test for detecting species associations, with some example applications. Ecology 65: 998–1005.

Schulz, M., and K. Stattegger. 1997. SPECTRUM: Spectral analysis of unevenly spaced paleoclimatic time series. Computational Geosciences 23:929–945.

Sommer, U., Z. M. Gliwicz, W. Lampert, and A. Duncan. 1986. The PEG model of seasonal succession of planktonic events in freshwaters. Archiv für Hydrobiologie 106:433–471.

Sommer, U., F. Sommer, B. Santer, E. Zöllner, K. Jürgens, C. Jamieson, M. Boersma, and K. Gocke. 2003. *Daphnia* versus copepod impact on summer phytoplankton: functional compensation at both trophic levels. Oecologia 135:639–647.

Steiner, C. F., Z. T. Long, J. A. Krumins, and P. J. Morin. 2005. Temporal stability of aquatic food webs: partitioning the effects of species diversity, species composition and enrichment. Ecology Letters 8:819–828.

Straile, D., and W. Geller. 1998. Crustacean zooplankton in Lake Constance from 1920 to 1995: Response to eutrophication and re-oligotrophication. Archiv für Hydrobiologie, Special Issues, Advances in Limnology 53:255–274.

Tilman, D. 1996. Biodiversity: population versus ecosystem stability. Ecology 77:350–363.

Tilman, D., C. L. Lehman, and C. E. Bristow. 1998. Diversity–stability relationships: statistical inevitability or ecological consequence? American Naturalist 151:277–282.

Van Voris, P., R. V. O'Neill, W. R. Emanuel, and H. H. Shugart, Jr. 1980. Functional complexity and ecosystem stability. Ecology 61:1352–1360.

Vasseur, D. A., U. Gaedke, and K. S. McCann. 2005. A seasonal alternation of coherent and compensatory dynamics occurs in phytoplankton. Oikos 110:507–514.

Yachi, S., and M. Loreau. 1999. Biodiversity and ecosystem functioning in a fluctuating environment: the insurance hypothesis. Proceedings of the National Academy of Science (USA) 96:1463–1468.

APPENDIX

Deriving thresholds for compensatory dynamics using the explained variance ratio (EVR) (*Ecological Archives* E088-122-A1).

Ecological Archives **E088-122-A1**

David A. Vasseur and Ursula Gaedke. 2007. Spectral analysis unmasks synchronous and compensatory dynamics in plankton communities. *Ecology* 88:2058–2071.

Appendix A. Deriving thresholds for compensatory dynamics using the explained variance ratio (EVR).

Consider the biomass contained in a community *C* which is comprised of *n* populations $P_1, P_2, \ldots, P_n$ each with variance $\sigma_{P_i}^2$.

Probability theory demonstrates that the community variance σ_C^2 is equal to the sum of all terms in the *n* by *n* variance-covariance matrix (Feller 1950), and since that matrix is symmetric we can write:

$$\sigma_C^2 = \sum_{i=1}^{n} \sigma_{P_i}^2 + 2\sum_{i}^{n}\sum_{j}^{i-1} \mathrm{cov}(i,j) \cdot \tag{A.1}$$

The variance ratio (*V*: Schluter 1984) is the ratio of this community variance to the sum of the population variances:

$$V = \frac{\sigma_C^2}{\sum_{i=1}^{n} \sigma_{P_i}^2} . \tag{A.2}$$

By combining expressions A.1 and A.2 it becomes clear that the variance ratio is equal to 1 when the sum of population covariances is zero (population dynamics are independent), whereas values greater (less) than 1 indicate positive (negative) covariances and thus synchronous (compensatory) dynamics amongst populations. The variance ratio reflects the cumulative population dynamics rather than the pair-wise dynamics; while some fraction of the *n* populations may be positively associated in time, another fraction could be negatively associated leading to cumulatively independent population dynamics.

We wish to derive a similar expression for the threshold between synchronous and compensatory dynamics which uses the metrics of our study, the variances of log-transformed population and community biomass data. Throughout our study we employ a comparison between community variance and the average population variance (or similarly the amounts of each explained by a certain frequency) which we call the explained variance ratio (EVR):

$$EVR_T = \frac{\sigma_{\log C}^2}{\sigma_{\log P}^2} \cdot \tag{A.3}$$

Doak et al. (1998) derived a relationship for the ratio between the community coefficient of variation ($CV_C = \sigma_C / \mu_C$) and the population coefficient of variation (CV_P) when population dynamics are independent (i.e., $V = 1$):

$$\frac{CV_C}{CV_P} = \frac{1}{\sqrt{n}} . \tag{A.4}$$

This relationship has since become known as the ‘Portfolio effect’, synonymous with the relationship known to economists. In this form it assumes that all populations have an equal *CV* and mean biomass (Tilman et al. 1998; Lhomme and Winkel 2002), however, Doak et al. (1998) also analyzed the relationship when populations differed in their mean biomasses. In this case, the first assumption (equal CV’s) only holds when the population variances scale as a power $z = 2$ of the population means ($\sigma_{P_i}^2 \propto \mu_{P_i}^{\ z}$). Tilman et al. (1998) and Lhomme and Winkel (2002) extended Doak et al.’s (1998) framework to include conditions when $z \neq 2$ and demonstrated that this introduces further assumptions about ‘overyielding’ in the community. However, retaining the assumption that $z = 2$ has an amenable property which allows us to employ Doak et al.’s (1998) framework; when $z = 2$ both the standard deviation of log-transformed data ($\sigma_{\log i}$) and its CV are independent of mean biomasses (McArdle et al. 1990). Although the two measures differ in magnitude, they scale in the same proportions, such that we can write:

$$\frac{CV_C}{CV_P} = \frac{\sigma_{\log C}}{\sigma_{\log P}} . \tag{A.5}$$

We can then define the threshold value for independent population dynamics of the EVR, using Eqs. A.3–A.5, as:

$$EVR_T = \frac{\sigma^2_{\log C}}{\sigma^2_{\log P}} = \frac{1}{n}\,. \tag{A.6}$$

To derive Eq. A.6, we have assumed that $z = 2$, however, the estimated values of z for the four communities used in this study range from 1.73 to 1.86 (Table 2). Assuming an over-estimate of z in our derivation makes the threshold for compensatory dynamics more conservative since $z < 2$ weakens the Portfolio effect (e.g., Cottingham et al. 2001).

Doak et al. (1998) provided an example describing how unevenness in the distribution of biomass amongst populations, a violation of the second assumption, alters this relationship. We adapt this expression to derive distinct values of the EVR_T for each of the four Lake Constance plankton communities. Doak et al. (1998) assumed that populations are ranked according to dominance and that successively ordered populations have mean abundances which decay according to:

$$\mu_i = \mu_1 \cdot e^{-a(i-1)} \tag{A.7}$$

where $a > 0$. Using Eq. 3 in Doak et al. (1998) the EVR_T for communities with an uneven biomass distribution becomes:

$$EVR_T = \frac{\left(1-e^{-a}\right)\left(1+e^{-an}\right)}{\left(1+e^{-a}\right)\left(1-e^{-an}\right)}\,. \tag{A.8}$$

Increases in the parameter a lead to increasing dominance of the community by few populations and to greater threshold values.

Since each of the Lake Constance communities differs in its evenness, we computed a specific threshold for each community by matching their observed evenness to the model (A.7). We determined the percentage of total community biomass that was contributed by the five dominant populations at each sampling event (Appendix Fig. A1). Since the evenness varies over time and we aim for conservative threshold values of the EVR, we chose the parameter a so that the contribution of the five dominant populations $\sum_i^5 \mu_i \Big/ \sum_i^\infty \mu_i$ was equal to the 25th percentile of the observed distribution. Appendix Fig. A2 shows how the EVR_T varies with richness for the values of a found to represent each of the four plankton communities. Using the fitted parameter a and the observed richness (Table 1) for each community we arrived at threshold values of $\mathrm{EVR}_T = 0.34$, 0.25, 0.14 and 0.16 for crustaceans, rotifers, phytoplankton and ciliates, respectively (cf. Table 2 and Fig. 4).

To summarize, by equating the EVR to previous theory deriving the expected reductions in variability associated with Portfolio effects, and by estimating the evenness of the biomass distribution for the four plankton communities we have derived thresholds for the EVR (EVR_T) which delimit communities dominated by synchronous dynamics (when the observed EVR is greater than EVR_T) from those dominated by compensatory dynamics (when the observed EVR is less than EVR_T).

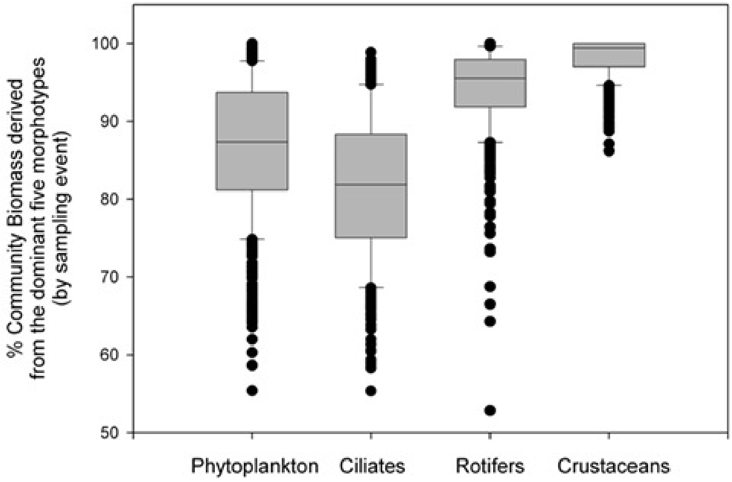

FIG. A1. The evenness of the four plankton communities in Lake Constance as shown by the percentage of community biomass contributed by the five dominant populations at each sampling date. The median, 25th and 75th percentiles are boxed, the whiskers represent the 10th and 90th percentiles and the outlying points are plotted as dots.

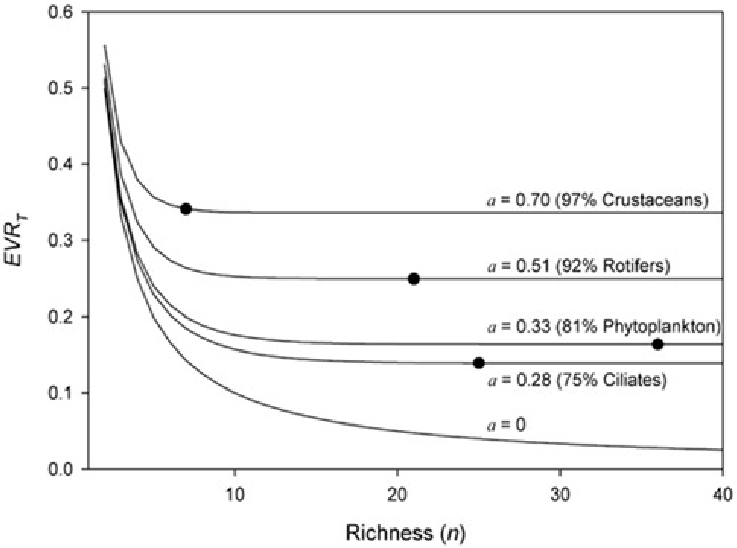

FIG. A2. The relationship between the EVR_T and richness from Eq. A.8. The four upper curves represent fitted values of the parameter a for the plankton communities in Lake Constance and the lower curve ($a = 0$; Eq. A.6) is provided for reference. The percentage of biomass contributed by the five dominant morphotypes for each community is shown in parentheses (note that this value is the 25th percentile from Appendix Fig. A1). The dots denote the values of EVR_T used for each community given their richness.

LITERATURE CITED

Cottingham, K. L., B. L. Brown, and J. T. Lennon. 2001. Biodiversity may regulate the temporal variability of ecological systems. Ecology Letters 4:72–85.

Doak, D. F., D. Bigger, E. K. Harding, M. A. Marvier, R. E. O'Malley, and D. Thomson. 1998. The statistical inevitability of stability-diversity relationships in community ecology. American Naturalist 151:264–276.

Feller, W. 1950. An introduction to probability theory and its application. Vol. 1. John Wiley and Sons. New York, New York, USA.

Lhomme, J. P., and T. Winkel. 2002. Diversity-stability relationships in community ecology: Re-examination of the portfolio effect. Theoretical Population Biology 62:271–279.

McArdle, B. H., K. J. Gaston, and J. H. Lawton. 1990. Variation in the size of animal populations: patterns, problems and artifacts. Journal of Animal Ecology 59:439–454.

[Back to E088-122]